STATISTICS, OPTIMIZATION AND INFORMATION COMPUTING
Stat., Optim. Inf. Comput., Vol. **15**, March 2026, pp 1834–1850.
Published online in International Academic Press (www.IAPress.org)

Impact of Fear, Allee Effects, and Harvesting on a Predator-Prey Delay Model with a Modified Beddington–DeAngelis Functional Response

Miswanto[1,*], Hasanur Mollah[2], Sahabuddin Sarwardi[2], Windarto[1], Eridani[1]

[1]*Department of Mathematics, Universitas Airlangga, Indonesia*
[2]*Department of Mathematics and Statistics, Aliah University, India*

Abstract This paper studies the dynamics of a delayed predator-prey model with a modified Beddington-DeAngelis response function influenced by fear factors, Allee effects, and harvesting on the predator population. This paper analyzes the influence of parameters, namely fear factors (ω), Allee effects (m), and delay time (τ), on the stability of the model's equilibrium point. First, an analysis of the existence of the model's equilibrium point is carried out, then an analysis of the stability and the influence of changes in the model's parameter values and delay time that can affect the stability of the model's equilibrium point is carried out. The analysis indicates that the larger the parameters ω, m, and τ, the more unstable the coexistence equilibrium point tends to be. Several numerical simulation results are used to validate the analytical results obtained.

Keywords Predator-prey model, Beddington–DeAngelis, Fear effects, Allee effect, Harvesting, Stability

AMS 2010 subject classifications 34C15, 34C23, 37G15, 37N25

DOI: 10.19139/soic-2310-5070-2574

1. Introduction

The study of predator-prey dynamics has become one of the main research topics in ecosystems, because it can provide a deep understanding of the influence of various ecological factors on ecosystem sustainability. In the ecosystem, the interaction between predators and prey is often influenced by external factors that can change the behavior of the predator-prey system dynamics as well as its stability and the sustainability of the ecosystem as a whole. The predator-prey model describes the dynamic interaction between two species with a pattern of relationships that influence each other and are often influenced by several factors, namely the fear experienced by the prey, the impact of the Allee effect on low populations, and hunting by the predator on the prey itself. To handle more realistic interactions in conditions of varying population densities, one of the functions that describes predator-prey interactions is the Beddington-DeAngelis function. This function describes the dynamics of predator–prey interactions in ecosystems that consider population density. Research on the combined effects of these factors is very important to understand how these elements interact with each other and affect the stability of the ecosystem in the long term.

Several researchers have studied these factors and the combination of these factors in the predator prey model. The fear effect, which reflects changes in prey behavior due to threats from predators, has been the focus of various studies. The importance of fear factors in prey populations has received special attention in several studies, where fear of predators can change prey behavior and significantly affect ecosystem structure. [1], [2] and [3] showed

*Correspondence to: Email: miswanto@fst.unair.ac.id.
Department of Mathematics, Universitas Airlangga, Jl. Mulyorejo, Surabaya, Indonesia.

ISSN 2310-5070 (online) ISSN 2311-004X (print)

that fear effects can produce bifurcations, dynamic oscillations, and changes in stability patterns in predator-prey models with Beddington–DeAngelis functional responses. In addition, these effects further enrich the dynamics of the model when combined with other factors such as non-linear harvesting, prey protection, or predator taxis, as described by [4], [5] and [6]. On the other hand, Allee effects, which usually occur in low-density populations, play an important role in ecosystem stability. Studies by [7] and [8] showed that Allee effects can introduce new bifurcation patterns and enrich population dynamics. In addition, Allee effects, which refer to the phenomenon where low population numbers can affect the survival or reproduction rate of a population, also play a role in population stability and sustainability in predator-prey models [9]. Meanwhile, [10] and [11] added that the combination of fear effects and Allee effects resulted in increasingly complex stability patterns. Beyond their short-term ecological impacts, the interaction of these factors may also provide insights into possible evolutionary implications, such as behavioral adaptations or shifts in reproductive strategies driven by prolonged exposure to fear and Allee effects.

Further studies by [12] and [13] showed that time delays in the predator-prey system, involving fear effects, Allee effects, and predator hunting cooperation, resulted in interesting Hopf bifurcations and oscillatory patterns. [14] and [15] showed that prey protection and predator taxis also contributed significantly to regulating the stability and bifurcation of the system. Furthermore, harvesting, both in predators and prey, has a major influence on ecosystem dynamics. Studies by [16] showed that harvesting strategies can significantly affect system stability. In [17], [18] and [19] highlighted that combining harvesting strategies with fear effects or Allee effects can produce rich bifurcation dynamics. While [20] and [21] showed that intraspecific competition and predator mortality rates that depend on prey density play important roles in determining dynamic patterns. [22] added that the reproductive Allee effect in the Leslie-Gower model can have significant implications for population stability. Hunting, as one of the factors that can have a direct impact on predator and prey populations, is often used in analyses to describe the influence of human activities on ecosystem balance [23] and [24].

Recent developments have focused on integrating these ecological components within unified modeling frameworks. For example, [25] explored a model incorporating fear, Allee effects, and periodic harvesting, uncovering complex bifurcation patterns. A review by [26] emphasized how integrated models are crucial for understanding ecological resilience. In [27], a predator–prey model with Allee effects and harvesting effort showed diverse bifurcation phenomena including Hopf and Bogdanov–Takens bifurcations. [28] studied memory effects in predators and fear in prey within a time-delayed model, revealing rich oscillatory dynamics. In a toxic environment context, [29] demonstrated that fear can significantly affect population dynamics, even in the absence of direct predation. Furthermore, Shao and Zhao [30] analyzed the stability and Hopf bifurcation of a delayed predator–prey system with fear and additional food, providing further insight into the complex interplay of ecological factors.

A relevant real-world example of these combined effects can be found in marine ecosystems, such as the interaction between sardines (Sardinella spp.) and tuna (Thunnus spp.). Fear effects occur when sardines reduce foraging activity to avoid predators, resulting in slower growth and reproduction. The Allee effect emerges when sardine abundance drops below a threshold, weakening schooling behavior and increasing vulnerability to predation[31]. Both species are also subject to commercial harvesting, and reproductive cycles introduce time delays in the response of predator populations to changes in prey abundance. This complex interplay closely reflects the ecological processes captured in our modified Beddington–DeAngelis predator–prey model.

This article examines the impact of fear, Allee effects, and harvesting in a predator-prey model with a Beddington–DeAngelis response function. This model allows to explore how these factors interact and influence the stability and dynamics of populations in an ecosystem. This research also includes an analysis of how an imbalance between predators and prey can arise as a result of excessive hunting or fear faced by the prey population [32]. Thus, the developed model provides a deeper understanding of the interactions between populations in more complex ecosystems. In this article, the combined impact of fear, Allee effects, and harvesting in a predator-prey model with a modified Beddington–DeAngelis response function is explored. Analytical and numerical approaches will be used to analyze these factors that influence the stability, bifurcation, and sustainability of the predator-prey model. In this paper, we study a predator-prey model with a modified Beddington–DeAngelis response function affected by fear, allee effects, predator harvesting, and time delays. We are interested in studying the stability of the equilibrium points of the model affected by these factors. In the next section, we present a predator-prey model

with a modified Beddington–DeAngelis response function. In section 3, we analyze the positivity and finiteness of the solution. In section 4, we investigate the existence and local stability of the equilibrium points of the model. In section 5, we investigate a bifurcation analysis representing a Hopf bifurcation for the proposed model. The last section presents numerical simulations to validate and further explore our analytical findings.

2. Model Assumptions and Formulation

This article examines the stability of a predator–prey model with a Beddington–DeAngelis response function, influenced by fear effects, Allee effects, nonlinear harvesting, and time delay. The model captures essential ecological dynamics such as inhibition, exploitation, predator saturation, and delayed predator reproduction. In constructing the model, several ecological and mathematical assumptions are made to ensure biological relevance and analytical tractability.

2.1. Model Assumptions

The model represents the interaction dynamics between two biological populations prey $x(t)$ and predator $y(t)$ using a system of nonlinear differential equations with time delay. The key assumptions underlying the model are:

- The populations $x(t)$ and $y(t)$ are assumed to be homogeneous, with no age structure or spatial distribution.
- The system is considered closed, with no immigration, emigration, or interaction with external populations.
- The time delay τ, representing predator gestation, is treated as fixed and deterministic, although real ecological systems may exhibit stochastic variation.
- The nonlinear rational form $\frac{x^2y^2}{a+bx^2+cy^2}$ captures a saturating predator functional response, where prey swarming behavior reduces predation efficiency at high prey densities.

These idealizations facilitate the analysis of dynamic behaviors such as stability, oscillations, and bifurcations. With appropriate parameter calibration, the model offers a biologically meaningful approximation for real-world predator-prey systems.

2.2. Model Formulation

The biological motivations behind each component of the model are as follows:

- **Fear effect:** Reduces the reproductive rate of the prey in response to predator presence, modeling behavioral stress or avoidance, as discussed in Yang & Jin (2022) [28].
- **Allee effect:** Incorporated additively in the prey's growth term to reflect lower reproduction at low population densities, based on Shao et al. (2024) [27].
- **Harvesting:** Predator harvesting is represented using a nonlinear saturating function $\frac{Ey}{1+\delta y}$, capturing diminishing returns at high predator densities, following Aldila & Adhyarini (2020) [25].
- **Predator functional response:** The interaction follows a modified Beddington–DeAngelis type functional response, incorporating prey protection, yielding a Holling type III form.

The original Beddington–DeAngelis functional response is:

$$f(x,y) = \frac{\beta xy}{a + bx + cy}$$

which is modified to account for prey protection as:

$$f(x,y) = \frac{\beta(1-n)x^2y^2}{a + bx^2 + cy^2}.$$

The nonlinear harvesting function applied to the predator population is:

$$\frac{Ey}{1+\delta y}.$$

2.2.1. Model Without Delay The predator–prey system without delay is given by:

$$\begin{aligned} \frac{dx}{dt} &= \frac{rx}{1+\omega y}\left(1-\frac{x}{K}\right)(x-m) - \frac{\beta_1 (1-n)\, x^2 y^2}{a+bx^2+cy^2} \\ \frac{dy}{dt} &= \frac{\beta_2 (1-n)\, x^2 y^2}{a+bx^2+cy^2} - \alpha_1 y - \alpha_2 y^2 - \frac{Ey}{1+\delta y}, \end{aligned} \tag{1}$$

where $x(t)$ and $y(t)$ denote the prey and predator population sizes at time t, respectively, and the initial conditions are $x(0) \geq 0$, $y(0) \geq 0$.

2.2.2. Model With Time Delay To reflect the biological delay in converting consumed prey into predator offspring (e.g., due to gestation), a discrete time delay τ is incorporated into the predator's growth term. The delayed model is formulated as:

$$\begin{aligned} \frac{dx}{dt} &= \frac{rx}{1+\omega y}\left(1-\frac{x}{K}\right)(x-m) - \frac{\beta_1 (1-n)\, x^2 y^2}{a+bx^2+cy^2} \\ \frac{dy}{dt} &= \frac{\beta_2 (1-n)\, x^2(t-\tau) y^2(t-\tau)}{a+bx^2(t-\tau)+cy^2(t-\tau)} - \alpha_1 y - \alpha_2 y^2 - \frac{Ey}{1+\delta y}, \end{aligned} \tag{2}$$

with initial conditions:

$$x(t) = \phi_1(t) \geq 0, \quad y(t) = \phi_2(t) \geq 0, \quad t \in [-\tau, 0].$$

Model Parameters The parameters of the model are defined as follows:

Table 1. Parameter definitions

Simbol	Deskripsi
r	Intrinsic growth rate of the prey population
K	Environmental carrying capacity for prey
ω	Level of fear effect experienced by prey
m	Allee threshold; if $x < m$, prey growth may become negative
β_1, β_2	Interaction and conversion rates between prey and predator
α_1	Natural death rate of the predator
α_2	Intraspecific competition-induced death rate in the predator
E	Harvesting effort
δ	Saturation parameter in the harvesting function
a, b, c	Parameters in the functional response
n	Prey protection factor
τ	Time delay representing predator gestation period

This model serves as a framework to analyze how various ecological and behavioral factors—such as fear, low-density effects, nonlinear harvesting, and reproductive delay—impact the stability and dynamics of predator–prey systems.

3. Basic properties of the model

In this section, the positive invariance and boundedness solution of the model are explained.

3.1. Positive Invariance

Proposition 1. *For the non-negative initial conditions* $(\phi_i, i = 1, 2)$*, defined on* $[0, +\infty)$*, there exists a non-negative solution of system* (2)*.*

Proof: We know that the survival of populations depends on the positivity of the system's solution. By integrating, it follows from the model (2) that

$$x(t) = x(0)exp\left(\int_0^t \left(\frac{rx}{1+\omega y}\left(1-\frac{x}{K}\right)(x-m) - \frac{\beta_1(1-n)x^2y^2}{a+bx^2+cy^2}\right)ds\right)$$

$$y(t) = y(0)exp\left(\int_0^t \left(\frac{\beta_2(1-n)x^2(t-\tau)y^2(t-\tau)}{a+bx^2(t-\tau)+cy^2(t-\tau)} - \alpha_1 y - \alpha_2 y^2 - \frac{Ey}{1+\delta y}\right)ds\right)$$

Hence, the solution $(x(t), y(t))$ of model (2) with initial condition $x(0) \geq 0$ and $y(0) \geq 0$ remains positive.

3.2. Boundedness

Theorem 2. *Prey and predator population of the system (2) is always bounded from above.*

Proof. Let $w = x(t-\tau) + \frac{\beta_1}{\beta_2}y$. For any $\eta > 0$ we have

$$\frac{dw}{dt} + \eta w = \frac{rx(t-\tau)}{1+\omega y(t-\tau)}\left(1-\frac{x(t-\tau)}{K}\right)(x(t-\tau)-m) - \frac{\beta_1}{\beta_2}\left(\alpha_1 y - \alpha_2 y^2 - \frac{Ey}{1+\delta y}\right)$$
$$+ \eta\left[x(t-\tau) + \frac{\beta_1}{\beta_2}y\right],$$
$$\leq rx(t-\tau)\left(1-\frac{x(t-\tau)}{k}\right)(x(t-\tau)-m) + \eta x(t-\tau) + \frac{\beta_1}{\beta_2}\left[(\eta-\alpha_1-E)y - \alpha_2 y^2\right]$$
$$\leq \frac{r\left[\left(K-m+\sqrt{(K-m)^2-3K(m-\eta)}\right)\left(K-m+\sqrt{(K-m)^2-3K(m-\eta)}\right)\left(K-m+\sqrt{(K-m)^2-3K(m-\eta)}\right)\right]^2}{27K} + \frac{m^2}{4\alpha_2}.$$

Then, $\frac{dw}{dt} + \eta w \leq M$

where $M = \frac{r\left[\left(K-m+\sqrt{(K-m)^2-3K(m-\eta)}\right)\left(K-m+\sqrt{(K-m)^2-3K(m-\eta)}\right)\left(K-m+\sqrt{(K-m)^2-3K(m-\eta)}\right)\right]^2}{27K} + \frac{m^2}{4\alpha_2}$

By use of Gronwall's inequality[36] application , we get

$$0 \leq w(t) \leq \frac{M}{\eta}\left(1-e^{-\eta t}\right) + w_1(0)e^{-\eta t}$$

Consequently, as $t \to \infty \implies 0 < w(t) < \frac{M}{\eta}$. This suggests that any solution for the systems represented by (2) is bounded.

4. Equilibria and their local stability

4.1. Equilibria

In this section, the existence of equilibrium points in the systems (2) is analyzed. Based on the analytical study, three equilibrium points were obtained, namely population extinction $(E_0(0,0))$ and predator-free equilibrium points $E_1(K,0)$ and $E_2(m,0)$. The equilibrium points were obtained based on the solution of:

$$\frac{rx}{1+\omega y}\left(1-\frac{x}{K}\right)(x-m) - \frac{\beta_1(1-n)x^2y^2}{a+bx^2+cy^2} = 0$$
$$\frac{\beta_2(1-n)x^2(t-\tau)y^2(t-\tau)}{a+bx^2(t-\tau)+cy^2(t-\tau)} - \alpha_1 y - \alpha_2 y^2 - \frac{Ey}{1+\delta y} = 0$$

The equilibrium point of coexistence, namely $E_*(x_*, y_*)$ is a solution to the equation above with $x_* \neq 0$ and $y_* \neq 0$. Basically, it is the intersection point in the positive quadrant of the system of equations above. Based on the system of equations above, it can be seen that the coexistence equilibrium point depends on the parameter values. Therefore, the system of equations above must be solved to obtain the coexistence equilibrium point, but it is impossible to show the analytical solution of the system of equations. Therefore, numerical calculations are needed to obtain the coexistence equilibrium point.

4.2. Analysis of local stability and bifurcations

Within this part, we examine the local stability of each of the system's four possible equilibrium points both with and without delay. Additionally, look into how the parameter τ, ω and m affects the system (2).

4.3. $E_0(0,0)$

The Jacobian matrix at $E_0(0,0)$, which is given by

$$J_{E_0} = \begin{bmatrix} -rm & 0 \\ 0 & -\alpha_1 - E \end{bmatrix}$$

The eigenvalues of this matrix are $-rm, -\alpha_1 - E$. Hence E_0 is always stable equilibrium point.

4.4. $E_1\,(K,0)$

The Jacobian matrix at E_1, which is given by

$$J_{E_1} = \begin{bmatrix} r\,(m - 2mK + K) & 0 \\ 0 & -\alpha_1 - E \end{bmatrix}$$

The eigenvalues of this matrix are $r\,(m - 2mK + K)$ and $-\alpha_1 - E$. The predator-free equilibrium point E_1 to the system (2) is asymptotically stable for all τ if $m + K < 2mK$ Otherwise, it will be unstable.

4.5. $E_2\,(m,0)$

The Jacobian matrix at E_2, which is given by

$$J_{E_2} = \begin{bmatrix} rm^2\left(2 - \frac{3}{K}\right) + rm & 0 \\ 0 & -\alpha_1 - E \end{bmatrix}$$

The eigenvalues of this matrix are $rm^2\left(2 - \frac{3}{K}\right) + rm$ and $-\alpha_1 - E$. The predator-free equilibrium point E_2 to the system (2) is asymptotically stable for all τ if $m\left(2 - \frac{3}{K}\right) + 1 < 0$ Otherwise, it will be unstable.

4.6. Co-existing equilibrium $E_*\,(x_*, y_*)$

The Jacobian matrix at E_*, which is given by

$$J_E = \begin{bmatrix} j_1 & j_2 \\ j_3 e^{-\lambda\tau} & j_4 + j_5 e^{-\lambda\tau} \end{bmatrix},$$

where

$$j_1 = \frac{r\left(-m + 2(1+m)x_* - \frac{3x_*^2}{K}\right)}{1 + \omega y_*} - \frac{2\beta_1\,(1-n)\,x_* y_*^2\left(a + cy_*^2\right)}{\left(a + bx_*^2 + cy_*^2\right)^2},$$

$$j_2 = -\frac{r\omega x_*}{(1+\omega y_*)^2}\left(1 - \frac{x_*}{k}\right)(x_* - m) - \frac{2\beta_1\,(1-n)\,x_*^2 y_*\left(a + bx_*^2\right)}{\left(a + bx_*^2 + cy_*^2\right)^2}$$

$$j_3 = \frac{2\beta_2\,(1-n)\,x_* y_*^2\left(a + cy_*^2\right)}{\left(a + bx_*^2 + cy_*^2\right)^2},\ j_4 = -\alpha_1 - 2\alpha_2 y_* - \frac{E}{(1+\delta y_*)^2}$$

$$j_5 = \frac{2\beta_2\,(1-n)\,x_*^2 y_*\left(a + bx_*^2\right)}{\left(a + bx_*^2 + cy_*^2\right)^2},$$

and λ is the characteristic value derived from the linearization of the delayed system.
Here, our primary goal is to examine how time delay affects the dynamic behaviour of system (2) at the interior

equilibrium point when prey and predators are present. The system's characteristic equation at E_* is as follows:

$$\lambda^2 + p_1\lambda + p_2 + (p_3\lambda + p_4)\, e^{-\lambda\tau} = 0, \tag{3}$$

where $p_1 = \dfrac{r\left(-m + 2(1+m)x_* - \frac{3x_*^2}{K}\right)}{1+\omega y_*} - \dfrac{2\beta_1(1-n)\,x_* y_*^2\left(a+cy_*^2\right)}{\left(a+bx_*^2+cy_*^2\right)^2} - \alpha_1 - 2\alpha_2 y_* - \dfrac{E}{(1+\delta y_*)^2}$

$$p_2 = \left(\frac{r\left(-m + 2(1+m)x_* - \frac{3x_*^2}{K}\right)}{1+\omega y_*} - \frac{2\beta_1(1-n)\,x_* y_*^2\left(a+cy_*^2\right)}{\left(a+bx_*^2+cy_*^2\right)^2}\right)\left(-\alpha_1 - 2\alpha_2 y_* - \frac{E}{(1+\delta y_*)^2}\right),$$

$$p_3 = -\frac{2\beta_2(1-n)\,x_*^2 y_*\left(a+bx_*^2\right)}{\left(a+bx_*^2+cy_*^2\right)^2}$$

$$p_4 = \left(\frac{r\left(-m + 2(1+m)x_* - \frac{3x_*^2}{K}\right)}{1+\omega y_*}\right)\left(\frac{2\beta_2(1-n)\,x_*^2 y_*\left(a+bx_*^2\right)}{\left(a+bx_*^2+cy_*^2\right)^2}\right)$$
$$+ \left(\frac{r\omega x_*}{(1+\omega y_*)^2}\left(1-\frac{x_*}{k}\right)(x_*-m)\right)\left(\frac{2\beta_2(1-n)\,x_* y_*^2\left(a+cy_*^2\right)}{\left(a+bx_*^2+cy_*^2\right)^2}\right).$$

Case I $(\tau = 0)$

When $\tau = 0$ that is, there is no time delay, the characteristic equation becomes

$$\lambda^2 + (p_1 + p_3)\,\lambda + p_2 + p_4 = 0, \tag{4}$$

The Routh-Hurwitz criteria is applied to the above equation (4), and E_* is asymptotically stable if the following condition holds $(H_1) : p_1 + p_3 > 0$ and $p_2 + p_4 > 0$.

Case II $(\tau > 0)$

To obtain the periodic solution of (1), we substitute $\lambda = i\sigma(\sigma > 0)$ in (3), and by equating the real and imaginary parts, we get the following equations:

$$p_4\cos\sigma\tau + p_3\sigma\sin\sigma\tau + p_2 = \sigma^2, \text{ and } p_3\sigma\cos\sigma\tau - p_4\sin\sigma\tau + p_1\sigma = 0 \tag{5}$$

$$\text{which gives} \quad \sigma^4 + \left(p_1^2 - 2p_2 - p_3^2\right)\sigma^2 + p_2^2 - p_4^2 = 0. \tag{6}$$

(H_2) : it is assumed that σ_* is a positive root of equation (3).
From above equations (5), we have

$$\tau_k = \frac{1}{\sigma_*}\arctan\left[\frac{\sigma_*\left(p_2p_3 - p_1p_4 - p_3\sigma_*^2\right)}{p_5p_3 + (p_2p_4 - p_4)\,\sigma_*^2}\right] + \frac{2k\pi}{\sigma_*}, \quad k = 0, 1, 2, 3...$$

We shall now examine the Hopf bifurcation's transversality condition. Differentiating of (3) with respect to τ and after simple calculations leads to

$$\Re\left[\frac{d\lambda}{d\tau}\right]^{-1}_{\lambda=i\sigma_*,\tau=\tau_*} = \frac{(2p_4 - p_1p_3)\,\sigma_*^2 cos\sigma_*\tau_* + \left(p_3\sigma_*^2 + p_1p_4\right)\sigma_*\sin\sigma_*\tau_* - p_3^2\sigma_*^2}{p_3^2\sigma_*^4 + p_4^2\sigma_*^2}.$$

Therefore, the transversality condition $\Re\left[\frac{d\lambda}{d\tau}\right]_{\lambda=i\sigma_*,\tau=\tau_*} > 0$ holds as if $(H_3) : (2p_4 - p_1p_3)\,\sigma_*^2 cos\sigma_*\tau_* + \left(p_3\sigma_*^2 + p_1p_4\right)\sigma_*\sin\sigma_*\tau_* - p_3^2\sigma_*^2 > 0$.
Thus, we can state the following theorem.

Theorem 3. *Suppose that the conditions* $(H_1), (H_2), (H_3)$ *hold for system* (1). *Interior equilibrium point* $E^*(x_*, y_*)$ *is locally asymptotically stable when* $\tau \in [0, \tau_*)$ *and a Hopf-bifurcation occurs at the equilibrium point* E^* *when* $\tau = \tau_*$.

5. Direction and stability of Hopf-bifurcation

In this section, we analyze the direction, stability, and period of the periodic solutions bifurcating from the positive equilibrium at the critical delay value $\tau = \tau_*$. The method we use is based on the center manifold theory and normal form calculation developed by Hassard et al. [33]. The following theorem summarizes the main results regarding the direction, stability, and period of the bifurcating periodic solutions.

Theorem 4. *If $\nu_1 > 0 (\nu_1 < 0)$ for the model system (1), then the Hopf bifurcation is supercritical (subcritical). The bifurcating periodic solutions are stable (unstable) if $\nu_2 < 0\,(\nu_2 > 0)$. The bifurcating periodic solutions increase (fall) if $T >, 0 (T < 0)$.The following parameters are derived in the proof:*

$$B_1(0) = \frac{i}{2\tau_*\sigma_*}\left(h_{11}h_{20} - 2|h_{11}|^2 - \frac{|h_{02}|^2}{3}\right) + \frac{h_{21}}{2},\ \nu_1 = -\frac{\Re(B_1(0))}{\Re(\lambda'(\tau_*))},$$
$$\nu_2 = 2\Re\left(B_1(0)\right),\ T = -\frac{\Im\left(B_1(0)\right) + \nu_1\Im(\lambda'(\tau_*))}{\tau_*\sigma_*}.$$

Proof: In keeping with Hassard's idea[33], the centre manifold theorem and normal form theory have been used to investigate the stability of bifurcated periodic solutions as well as the direction of the Hopf bifurcation.
Let $\tau = \tau_* + \eta, \eta \in R$, then $\eta = 0$ is the Hopf bifurcation value of system (1). Rescaling the time delay $t \to (\frac{t}{\tau})$, then system (1) can be re-written as

$$\dot{w}(t) = L_\eta w_t + f(\eta, w_t), \tag{7}$$

where $w(t) = (w_1(t), w_2(t))^T \in R^3, w_t(\theta) = w(t+\theta)$ and $L_\mu : C \to R^3, f : R \times C \to R^3$ are given by

$$L_\eta w_t = (\tau_* + \eta)\begin{pmatrix} j_1 & j_2 \\ 0 & j_4 \end{pmatrix}\begin{pmatrix} w_{1t}(0) \\ w_{2t}(0) \end{pmatrix} + (\tau_* + \eta)\begin{pmatrix} 0 & 0 \\ j_3 & j_5 \end{pmatrix}\begin{pmatrix} w_{1t}(-1) \\ w_{2t}(-1) \end{pmatrix}, \tag{8}$$

$$f(\eta, w_t) = (\tau_* + \eta)\begin{pmatrix} a_{30}w_{1t}^3(0) + a_{11}w_{1t}(0)w_{2t}(0) + a_{21}w_{1t}^2(0)w_{2t}(0) + \dots \\ b_{30}w_{1t}^3(-1) + b_{11}w_{1t}(-1)w_{2t}(-1) + b_{02}w_{2t}^2(-1) + \dots \end{pmatrix} \tag{9}$$

where

$$a_{11} = -\frac{r\omega\left(-m + 2(1+m)x_* - \frac{3x_*^2}{K}\right)}{\left(1+\omega y_*\right)^2} + \frac{4\beta_1\left(1-n\right)x_*y_*\left(a + 2cy_*^2\right)}{\left(a + bx_*^2 + cy_*^2\right)^2}$$
$$- \frac{8\beta_1 c\left(1-n\right)x_*y_*^3\left(a + cy_*^2\right)}{\left(a + bx_*^2 + cy_*^2\right)^3},\ a_{21} = -\frac{r\omega\left(2(1+m) - \frac{6x_*}{K}\right)}{\left(1+\omega y_*\right)^2} + \frac{4\beta_1\left(1-n\right)y_*\left(a + 2cy_*^2\right)}{\left(a + bx_*^2 + cy_*^2\right)^2}$$
$$+ \frac{48bc\beta_1\left(1-n\right)x_*^2y_*^3\left(a + cy_*^2\right)}{\left(a + bx_*^2 + cy_*^2\right)^4} - \frac{8\beta_1\left(1-n\right)y_*\left[2bx_*^2\left(a + 2cy_*^2\right) + cy_*^2\left(3a + 5cy_*^2\right)\right]}{\left(a + bx_*^2 + cy_*^2\right)^3}$$
$$a_{12} = \frac{r\omega^2\left(-m + 2(1+m)x_* - \frac{3x_*^2}{K}\right)}{\left(1+\omega y_*\right)^2} - \frac{8\beta_1 c\left(1-n\right)x_*y_*^2\left[2\left(a + 2cy_*^2\right) + y_*^2\left(3a + 5cy_*^2\right)\right]}{\left(a + bx_*^2 + cy_*^2\right)^3}$$

$$+\frac{4\beta_1(1-n)x_*\left(a+6cy_*^2\right)}{\left(a+bx_*^2+cy_*^2\right)^2}+\frac{48c^2\beta_1(1-n)x_*y_*^4\left(a+cy_*^2\right)}{\left(a+bx_*^2+cy_*^2\right)^4},\ a_{20}=-\frac{6rx_*}{K(1+\omega y_*)}$$

$$+\frac{2\beta_1(1-n)y_*^2\left(a+cy_*^2\right)}{\left(a+bx_*^2+cy_*^2\right)^2}-\frac{8b\beta_1(1-n)x_*^2y_*\left(a+cy_*^2\right)}{\left(a+bx_*^2+cy_*^2\right)^3},\ a_{30}=-\frac{6r}{K(1+\omega y_*)}$$

$$-\frac{24b\beta_1(1-n)x_*y_*^2\left(a+cy_*^2\right)}{\left(a+bx_*^2+cy_*^2\right)^3}+\frac{48b^2\beta_1(1-n)x_*^3y_*^2\left(a+cy_*^2\right)}{\left(a+bx_*^2+cy_*^2\right)^4}$$

$$a_{02}=\frac{2r\omega^2x_*}{(1+\omega y_*)^3}\left(1-\frac{x_*}{k}\right)(x_*-m)+\frac{2\beta_1(1-n)x_*^2\left(a+bx_*^2\right)}{\left(a+bx_*^2+cy_*^2\right)^2}-\frac{8c\beta_1(1-n)x_*^2y_*\left(a+bx_*^2\right)}{\left(a+bx_*^2+cy_*^2\right)^3}$$

$$a_{03}=-\frac{6r\omega^3x_*}{(1+\omega y_*)^4}\left(1-\frac{x_*}{k}\right)(x_*-m)-\frac{24c\beta_1(1-n)y_*x_*^2\left(a+bx_*^2\right)}{\left(a+bx_*^2+cy_*^2\right)^3}+\frac{48c^2\beta_1(1-n)y_*^3x_*^2\left(a+bx_*^2\right)}{\left(a+bx_*^2+cy_*^2\right)^4}$$

$$b_{11}=\frac{4\beta_2(1-n)x_*y_*\left(a+2cy_*^2\right)}{\left(a+bx_*^2+cy_*^2\right)^2}-\frac{8\beta_2c(1-n)x_*y_*^3\left(a+cy_*^2\right)}{\left(a+bx_*^2+cy_*^2\right)^3}$$

$$b_{21}=\frac{4\beta_2(1-n)y_*\left(a+2cy_*^2\right)}{\left(a+bx_*^2+cy_*^2\right)^2}+\frac{48bc\beta_2(1-n)x_*^2y_*^3\left(a+cy_*^2\right)}{\left(a+bx_*^2+cy_*^2\right)^4}$$

$$-\frac{8\beta_2(1-n)y_*\left[2bx_*^2\left(a+2cy_*^2\right)+cy_*^2\left(3a+5cy_*^2\right)\right]}{\left(a+bx_*^2+cy_*^2\right)^3}$$

$$b_{12}=\frac{4\beta_2(1-n)x_*\left(a+6cy_*^2\right)}{\left(a+bx_*^2+cy_*^2\right)^2}+\frac{48c^2\beta_2(1-n)x_*y_*^4\left(a+cy_*^2\right)}{\left(a+bx_*^2+cy_*^2\right)^4}$$

$$-\frac{8\beta_2c(1-n)x_*y_*^2\left[2\left(a+2cy_*^2\right)+y_*^2\left(3a+5cy_*^2\right)\right]}{\left(a+bx_*^2+cy_*^2\right)^3}$$

$$b_{20}=\frac{2\beta_2(1-n)y_*^2\left(a+cy_*^2\right)}{\left(a+bx_*^2+cy_*^2\right)^2}-\frac{8b\beta_2(1-n)x_*^2y_*\left(a+cy_*^2\right)}{\left(a+bx_*^2+cy_*^2\right)^3}$$

$$b_{30}=-\frac{24b\beta_2(1-n)x_*y_*^2\left(a+cy_*^2\right)}{\left(a+bx_*^2+cy_*^2\right)^3}+\frac{48b^2\beta_2(1-n)x_*^3y_*^2\left(a+cy_*^2\right)}{\left(a+bx_*^2+cy_*^2\right)^4}$$

$$b_{02}=\frac{2\beta_2(1-n)x_*^2\left(a+bx_*^2\right)}{\left(a+bx_*^2+cy_*^2\right)^2}-\frac{8c\beta_2(1-n)x_*^2y_*\left(a+bx_*^2\right)}{\left(a+bx_*^2+cy_*^2\right)^3}$$

$$b_{03}=-\frac{24c\beta_2(1-n)y_*x_*^2\left(a+bx_*^2\right)}{\left(a+bx_*^2+cy_*^2\right)^3}+\frac{48c^2\beta_2(1-n)y_*^3x_*^2\left(a+bx_*^2\right)}{\left(a+bx_*^2+cy_*^2\right)^4}$$

$$c_{02}=-\alpha-\frac{E}{(1+\delta y_*)^3},\ c_{03}=-\frac{E}{(1+\delta y_*)^4}$$

According to Riesz representation theorem [34], there exists a 2×2 matrix $\mu(\theta,\eta),\theta\in[-1,0]$, such that

$$L_\eta\phi=\int_{-1}^{0}d\mu(\theta,\eta)\phi(\theta),\ \text{for}\ \phi\in C=C([-1,0],R^3),\tag{10}$$

In fact we can choose

$$\mu(\theta,\eta)=(\tau_*+\eta)\begin{bmatrix}j_1 & j_2\\ 0 & j_4\end{bmatrix}\delta(\theta)+(\tau_*+\eta)\begin{bmatrix}0 & 0\\ j_3 & j_5\end{bmatrix}\delta(\theta+1),\tag{11}$$

where δ is the Dirac delta function. For $\phi \in C([-1,0], R^3)$, define

$$A_1(\eta)\phi = \begin{cases} \frac{d\phi(\theta)}{d\theta}, & -1 \le \theta < 0 \\ \int_{-1}^{0} d\mu(\theta,\eta)\phi(\theta), & \theta = 0 \end{cases} \quad \text{and} \quad A_2(\eta)\phi = \begin{cases} 0 & -1 \le \theta < 0, \\ f(\eta,\phi) & \theta = 0. \end{cases} \tag{12}$$

Then (1) is equivalent to the abstract differential equation

$$\dot{w}(t) = A_1\eta w_t + A_2(\eta)w_t, \text{ where } w_t(\theta) = w(t+\theta),\ \theta \in [-1,0] \tag{13}$$

$$\text{For } \psi \in C^1([0,1],(R^2)^*), \text{ define } A_1^*\psi(s) = \begin{cases} -\frac{d\psi(s)}{ds} & 0 < s \le 1, \\ \int_{-1}^{0} d\eta^T(s,0)\psi(-s) & s = 0. \end{cases} \tag{14}$$

For $\phi \in C([0,1], R^2)$ and $\psi \in C^1([0,1],(R^3)^*)$, define a bilinear inner product

$$< \psi, \phi >= \bar{\psi}(0)\phi(0) - \int_{-1}^{0}\int_{\xi=0}^{\theta} \psi^T(\xi-\theta)d\eta(\theta)\phi(\xi)d\xi, \tag{15}$$

where $\mu(\theta) = \mu(\theta,0), A_1 = A_1(0)$ and A^* are adjoint operators. Here $\pm i\sigma_*\tau_*$ are the eigenvalues of $A_1(0)$, and they are also eigenvalues of A_1^*. Here $S(\theta) = (1,\gamma_1)^T e^{i\sigma_*\tau_*\theta}$ $(\theta \in [-1,0])$ and $S^*(q) = \frac{1}{D}(1,\gamma_1^*)^T e^{i\sigma_*\tau_* q}$ $(q \in [-1,0])$ are the eigenvectors of $A_1(0)$ and A_1^* corresponding to the eigenvalues $i\sigma_*\tau_*$ and $-i\sigma_*\tau_*$ respectively. Then $A_1(0)S(\theta) = i\tau_*\sigma_*S(\theta)$. Then it follows from the definition of $A_1(0)$ and A_1^* in 11, (12), 13 and using a computation process similar to Song and Wei [35], we obtain

$$\gamma_1 = \frac{b_{21}e^{-i\sigma_*\tau_*}}{i\sigma - a_{22} - b_{22}e^{-i\sigma_*\tau_*}},\ \gamma_1^* = -\frac{b_{21}}{b_{22} + (a_{11}+i\sigma)\,e^{-i\sigma_*\tau_*}},.$$

In order to assure that $< S^*(q), S(\theta) >= 1$ and $< S^*(q), \bar{S}(\theta) >= 0$, we need to determine the value of D. Hence, from $< S^*(q), S(\theta) >= 1$, we have

$$\bar{D} = 1 + \gamma_1\bar{\gamma_1^*} + \tau_* e^{-i\sigma_*\tau_*}\left(b_{22}\gamma_1\gamma_1^* + b_{21}\gamma_1^*\right). \tag{16}$$

Following the algorithm explained in Hassard[33] and using a computation process similar to Song and Wei [35], which is used to obtain the properties of Hopf-bifurcation, we obtain

$$\begin{aligned}
h_{20} &= \frac{\tau_*}{\bar{D}}\left[a_{20} + \gamma_1^2 a_{02} + \gamma_1 a_{11} + \bar{\gamma_1^*}\left[e^{-2i\sigma_*\tau_*}\left(b_{11}\gamma_1 + b_{20} + b_{02}\gamma_1^2\right) + \gamma_1^2 c_{02}\right]\right].\\
h_{11} &= \frac{\tau_*}{\bar{D}}\left[2a_{20} + 2\gamma_1\bar{\gamma_1}a_{02} + a_{11}\left(\gamma_1 + \bar{\gamma_1}\right) + \bar{\gamma_1^*}\left(2b_{20} + 2\gamma_1\bar{\gamma_1}(b_{02}+c_{02}) + b_{11}\left(\gamma_1 + \bar{\gamma_1}\right)\right)\right].\\
h_{02} &= \frac{\tau_*}{\bar{D}}\left[a_{20} + \bar{\gamma_1}^2 a_{02} + \bar{\gamma_1}a_{11} + \bar{\gamma_1^*}\left[e^{-2i\sigma_*\tau_*}\left(b_{11}\bar{\gamma_1} + b_{20} + b_{02}\bar{\gamma_1}^2\right) + \bar{\gamma_1}^2 c_{02}\right]\right]\\
h_{21} &= \frac{\tau_*}{\bar{D}}\left[3a_{30} + a_{11}\left(W_{11}^{(2)}(0) + \frac{1}{2}W_{20}^{(2)}(0) + \frac{1}{2}\bar{\gamma_1}W_{20}^{(1)}(0) + \gamma_1 W_{11}^{(1)}(0)\right) + 3\gamma_1^2\bar{\gamma_1}a_{03}\right.\\
&\quad + a_{20}\left(2W_{11}^{(1)}(0) + W_{20}^{(1)}(0)\right) + a_{02}\left(2\gamma_1 W_{11}^{(2)}(0) + \bar{\gamma_1}W_{20}^{(2)}(0)\right) + a_{21}\left(2\gamma_1 + \bar{\gamma_1}\right)\\
&\quad \left. + a_{12}\left(2\gamma_1\bar{\gamma_1} + \gamma_1^2\right) + \bar{\gamma_1^*}3e^{-i\sigma_*\tau_*}\left(b_{30} + \gamma_1^2\bar{\gamma_1}b_{03}\right) + \bar{\gamma_1^*}b_{02}\left(2W_{11}^{(2)}(-1)e^{-i\sigma_*\tau_*} + W_{20}^{(2)}(-1)e^{i\sigma_*\tau_*}\right)\right.
\end{aligned}$$

$$+\bar{\gamma_1^*}b_{20}\left(2W_{11}^{(1)}(-1)e^{-i\sigma_*\tau_*}+W_{20}^{(1)}(-1)e^{i\sigma_*\tau_*}\right)+\bar{\gamma_1^*}b_{21}e^{-i\sigma_*\tau_*}\left(\bar{\gamma_1}+2\gamma_1\right)$$
$$+\bar{\gamma_1^*}b_{12}e^{-i\sigma_*\tau_*}\left(2\gamma_1\bar{\gamma_1}+\gamma_1^2\right)+b_2\bar{\gamma_1^*}\left(2\gamma_1W_{11}^{(2)}(0)+\bar{\gamma_1}W_{20}^{(2)}(0)\right)+3\bar{\gamma_1^*}\gamma_1\bar{\gamma_1}c_{03}$$
$$+\bar{\gamma_1^*}b_{11}\left(e^{-i\omega_*\tau_*}\left(\gamma_1W_{11}^{(1)}(-1)+W_{11}^{(2)}(-1)\right)+\frac{1}{2}e^{-i\omega_*\tau_*}\left(\bar{\gamma_1}W_{20}^{(1)}(-1)+\frac{1}{2}W_{20}^{(2)}(-1)\right)\right)\Bigg].$$

where $W_{20}(\theta)=\dfrac{ih_{20}}{\omega_*\tau_*}S(0)e^{i\theta\omega_*\tau_*}+\dfrac{i\bar{h}_{02}}{3\omega_*\tau_*}\bar{S}(0)e^{-i\theta\omega_*\tau_*}+C_1e^{2i\theta\omega_*\tau_*},$

$W_{11}(\theta)=-\dfrac{ih_{11}}{\omega_*\tau_*}S(0)e^{i\theta\omega_*\tau_*}+\dfrac{i\bar{h}_{11}}{\omega_*\tau_*}\bar{S}(0)e^{-i\theta\omega_0\tau_0}+C_2,$

and $C_1=(C_1^1,C_1^2)^T$, and $C_2=(C_2^1,C_2^2)^T$ both are constant vectors in R^2. After calculation, we get $C_1=2D_1^{-1}D_2$ and $C_2=2D_3^{-1}D_4$ with

$$D_1=\begin{bmatrix}2i\omega_*-a_{11} & -a_{12}\\ -b_{21} & 2i\omega_*-a_{22}\end{bmatrix},\quad D_2=\begin{bmatrix}a_{20}+\gamma_1^2a_{02}+\gamma_1a_{11}\\ e^{-2i\omega_*\tau_*}\left(b_{11}\gamma_1+b_{20}+b_{02}\gamma_1^2\right)+\gamma_1^2c_{02}\end{bmatrix},$$
$$D_3=\begin{bmatrix}-a_{11} & -a_{12}\\ -a_{21} & -a_{22}\end{bmatrix},\quad D_4=\begin{bmatrix}2a_{20}+2\gamma_1\bar{\gamma_1}a_{02}+a_{11}\left(\gamma_1+\bar{\gamma_1}\right)\\ e^{-2i\omega_*\tau_*}\left(b_{11}\bar{\gamma_1}+b_{20}+b_{02}\bar{\gamma_1}^2\right)+\bar{\gamma_1}^2c_{02}\end{bmatrix}.$$

Therefore, each h_{ij} can be expressed by the parameters and delay. Thus, we compute the following values:

$$B_1(0)=\frac{i}{2\tau_*\omega_*}\left(h_{11}h_{20}-2|h_{11}|^2-\frac{|h_{02}|^2}{3}\right)+\frac{h_{21}}{2},\ \nu_1=-\frac{\Re(B_1(0))}{\Re(\lambda'(\tau_*))},$$
$$\nu_2=2\Re\left(B_1(0)\right),\ T=-\frac{\Im\left(B_1(0)\right)+\nu_1\Im(\lambda'(\tau_*))}{\tau_*\omega_*}.$$

All constants such as $B_1(0)$ are computed explicitly using the center manifold function W, its derivatives, and the nonlinear terms in $f(\eta,w_t)$, following the formulas in Hassard et al. [32]. This concludes the theoretical derivation of the Hopf bifurcation properties. In the next section, we verify these analytical results via numerical simulations.

6. Numerical simulation

Using the MATLAB programme, we run a few numerical simulations in this part to validate and expand on our analytical result. Taking default values of following set of parameters, say Q1: $r=3.0, K=2, n=0.1, a=0.2, b=0.2, c=1.0, \beta_1=1.1, \beta_2=1.8, \alpha_1=0.2, \alpha_2=1.2, \delta=0.8, E=0.3$ with starting point $x(0)=y(0)=1$.

The parameters τ (gestation time delay), ω (cost of fear) and m (Allee factor) will vary during the computational simulations. Taking $\tau=1.0, \omega=2.8, m=0.1$ with the collection of parameters value Q1, there exists a co-existing equilibrium point $E_*(0.9539, 2.473)$. Additionally, meet the requirements in Theorem 5.1, and we'll be able to determine the critical delay of $\tau=0.96$, at which a Hopf-bifurcation displays itself. Accordingly, the system (1) is unstable if $\tau=1.4>0.96$ (see Figure 2) and asymptotically stable at E^* for $\tau=0.8<0.96$ (see Figure 1). For the set of parameters values Q1, the parameteric bifurcation diagram for all populations is shown in Figure 3, and it displays the way the system evolves when τ's numerical values fluctuate within $[0.7, 1.3]$. It suggests that the behaviour of the system will fluctuate via a Hopf bifurcation point at $\tau_*=0.98$ if we raise the value of the τ parameter.

Now, in the presence of a time delay, the set of parameters chosen in Q1 with the initial condition $x(0)=y(0)=1$ while setting fear factor (ω) as the bifurcation parameter. Now preserving values of other parameters in Q1 with $\tau=1.2, m=0.1$, and for $\omega=2$ the co-existing equilibrium point $E_*(0.9539, 2.473)$ is

asymptotically stable, which is shown in Figure 4. Now if we increase the value of parameter ω, then for system (2) leads to a Hopf-bifurcation and critical value of ω is $\omega_* = 2.45$. Further increment in the value of ω then system becomes unstable, which is shown in Figure 5. For the provided set of factors values Q1 with $m = 0.1$, Figure 6's parameteric bifurcation diagram for all populations shows how the system evolves when ω's numerical values oscillate within $[2.0, 3.2]$ in the presence fixed gestation time delay $\tau = 1.2$. It is anticipated that changes in the ω parameter would result in behavioural oscillations in the system via a Hopf bifurcation point at $\omega^* = 2.45$.

Similarly setting Allee factor (m) as the bifurcation parameter. Now preserving values of other parameters in Q1 with $\tau = 0.9, \omega = 3.2$, and for $m = 0.05$ the co-existing equilibrium point $E_*(0.9539, 2.473)$ is asymptotically stable, which is shown in Figure 7. Now if we increase the value of parameter m, then for system (2) leads to a Hopf-bifurcation and critical value of m is $m_* = 0.07$. Further increment in the value of m then system becomes unstable, which is shown in Figure 9. For the provided set of factors values Q1 with $\omega = 3.2$, Figure 9's parameteric bifurcation diagram for all populations shows how the system evolves when ω's numerical values oscillate within $[0.05, 0.15]$ in the presence fixed gestation time delay $\tau = 0.9$. It is anticipated that changes in the m parameter would result in behavioural oscillations in the system via a Hopf bifurcation point at $m^* = 0.07$. In addition, Figures 10 and 11 demonstrate the effects of increasing the harvesting parameter E while keeping $\tau = 0.9$ fixed; initially at $E = 0.4$, the coexistence equilibrium E_* remains stable, but as E increases to 0.9, the equilibrium loses stability and the system exhibits sustained periodic oscillations. This transition is evidenced by the phase portrait in Figure 10, where trajectories spiral away from E_* to form a stable limit cycle, and by the time series in Figure 11 showing persistent oscillations in prey and predator populations. These results indicate that increases in E, like variations in m, can induce a Hopf bifurcation, causing the system to shift from a stable equilibrium to stable cyclic dynamics.

7. Conclusion

Predator harvest, Allee effects, and prey fear of predators are the three components that are considered in this article's analysis of a predator-prey model with a Beddington–DeAngelis response function. Additionally, a time delay that represents the predator's gestation delay is included.

We determined the presence of equilibria and given their positive conditions for the suggested delayed model (2). There are four potential non-negative equilibria in this prey-predator model, and we also offer a thorough examination of the stability of each of these systems. Because both prey and predator populations are originally available, E_0 is always stable among them. We see that equilibrium point E_1 of the system (2) is asymptotically stable for all τ if $m + K < 2mK$. Otherwise, it will be unstable. Also, equilibrium point E_2 of the system (2) is asymptotically stable for all τ if $m\left(2 - \frac{3}{K}\right) + 1 < 0$. Otherwise, it will be unstable.

We have obtained the sufficient and necessary conditions for the stability and instability of the interior equilibrium when $\tau = 0$ as well as when $\tau > 0$. It has been shown that, under some conditions, the time delay τ may destabilise the co-existing equilibrium of the system (2) and cause the population to fluctuate. The system (2) undergoes a Hopf-bifurcation, and it is discovered that the system is locally asymptotically stable when the time delay is sufficiently minimal. When there is a fixed gestation time delay, we looked at the fear effect that predators concurrently impose on prey species. Hopf-bifurcation is experienced by the delayed system (2), and its critical value is ω_*, where Hopf-bifurcation takes place at E_*. In this case, the delayed system is unstable if $\omega > \omega_*$. As ω decreases below ω_*, the system stabilises and remains stable for further decreases in ω.

Similarly, with a fixed gestation time delay and a fixed value of the fear parameter, we examined the Allee effect imposed on prey species. The Allee parameter m destabilises the co-existing equilibrium of the system (2) and causes the population to fluctuate. Hopf-bifurcation is experienced by the delayed system (2), and its critical value is m_*, where Hopf-bifurcation takes place at E_*. In this case, the delayed system is unstable if $m > m_*$. As m

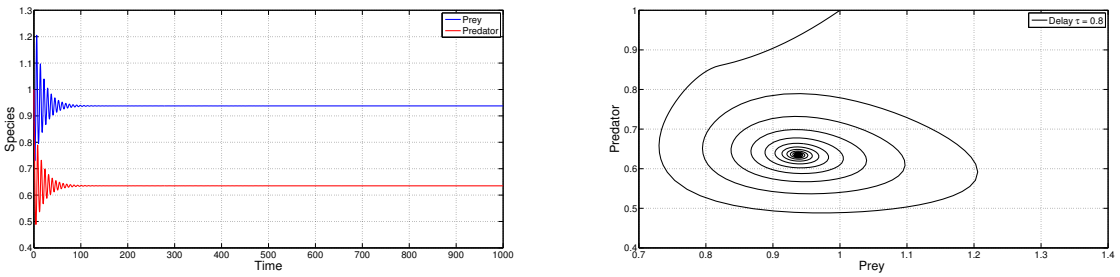

(a) (b)

Figure 1. Show that for the set of parameters chosen in Q1 with starting point $x(0) = y(0) = 1$, E_* is locally asymptotically stable when $\tau = 0.8(< 0.96 = \tau_*)$. (a) The solution graph of x, and y of the system (2). (b) The phase space graph of the system (2).

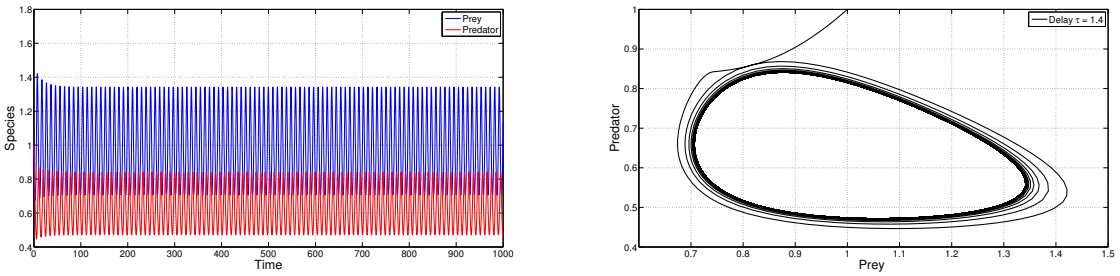

(a) (b)

Figure 2. For the set of parameters chosen in Q1 with starting point $x(0) = y(0) = 1$, the coexistence equilibrium E_* loses its stability when $\tau = 1.4(> 0.96 = \tau_*)$. Both the Figures (a) and (b) display periodic oscillations and ultimately a stable limit cycle around the E_* when $\tau = 1.4$.

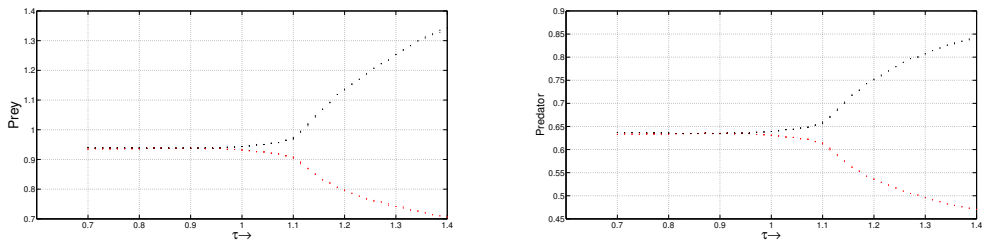

(a) (b)

Figure 3. Diagram illustrating the prey and predator populations' bifurcation in terms of delay with respect to the bifurcating parameter, τ (bifurcation at $\tau_* = 0.96$)for the parameter set Q1 with starting point $x(0) = y(0) = 1$.

decreases below m_*, the system stabilises and remains stable for further decreases in m.

Although evolutionary processes are not explicitly included in the current model, the dynamics revealed in this study, particularly those driven by prolonged fear effects and strong Allee thresholds, impact prey evolution. Long-term exposure to predation risk may lead to behavioral or reproductive adaptations in prey populations, while persistent Allee effects may influence the evolution of group behavior or reproductive strategies. These aspects are beyond the scope of the current analysis but provide meaningful directions for future research aimed at

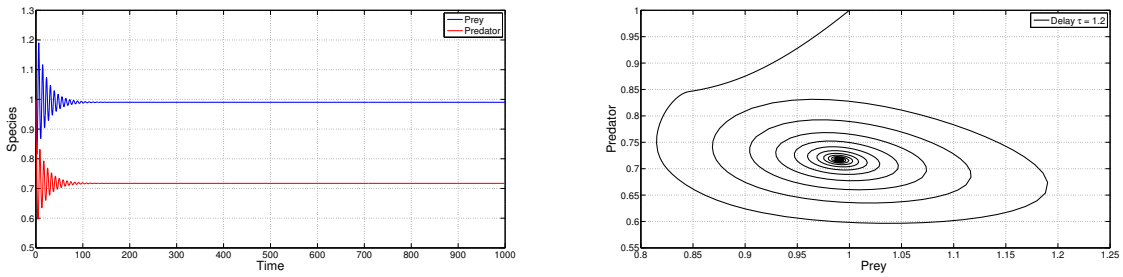

(a) (b)

Figure 4. Taking $\tau = 1.2$ with value of parameters chosen in Q1 with starting point $x(0) = y(0) = 1$, E_* is locally asymptotically stable when fear term $\omega = 2(< 2.45 = \omega_*)$. (a) The solution graph of x, and y of the system (2). (b) The phase space graph of the system (2).

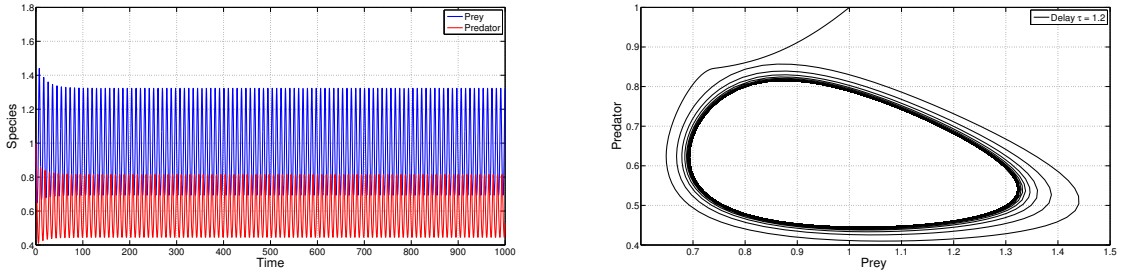

(a) (b)

Figure 5. Taking $\tau = 1.2$ with value of parameters chosen in Q1 with starting point $x(0) = y(0) = 1$,, the coexistence equilibrium E_* loses its stability when $\omega = 3.2(> 2.45 = \omega_*)$. Both the Figures (a) and (b) display periodic oscillations and ultimately a stable limit cycle around the E_*.

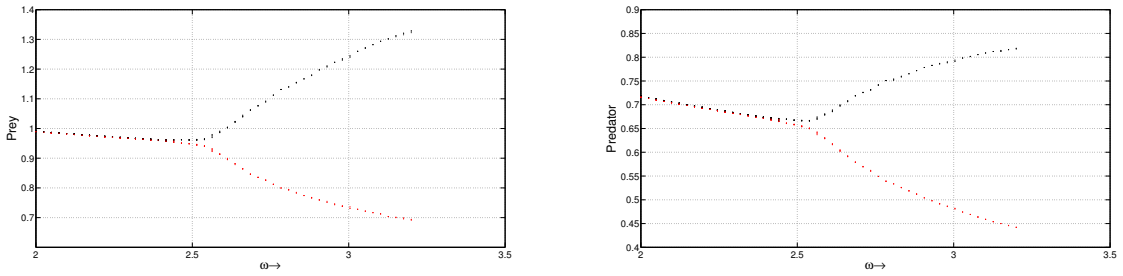

(a) (b)

Figure 6. Diagram illustrating the prey and predator populations' bifurcation in terms of fear factor with respect to the bifurcating parameter, ω (bifurcation at $\omega_* = 2.45$)for the parameter set Q1 with starting point $x(0) = y(0) = 1$.

bridging ecological dynamics with evolutionary theory.

The findings of this study have important implications for ecological management, such as designing sustainable harvesting strategies and understanding population persistence under predation risk and Allee effects. Incorporating these factors into management plans could help maintain ecosystem stability.

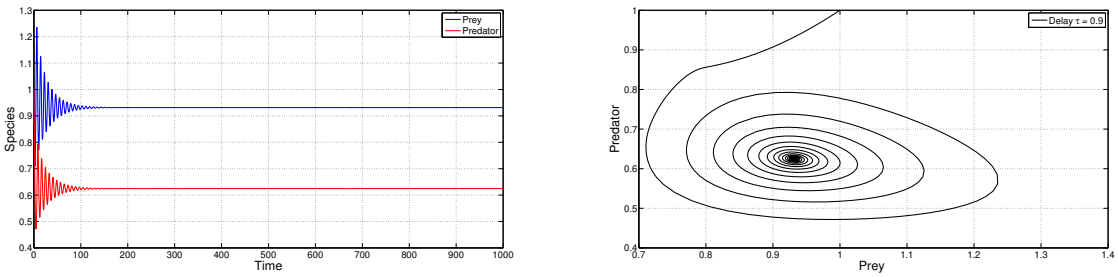

(a) (b)

Figure 7. Taking $\tau = 0.9, \omega = 3.2$ with value of parameters chosen in Q1 with starting point $x(0) = y(0) = 1$, E_* is locally asymptotically stable when Allee effect $m = 0.05 (< 0.07 = m_*)$. (a) The solution graph of x and y of the system (2). (b) The phase space graph of the system (2).

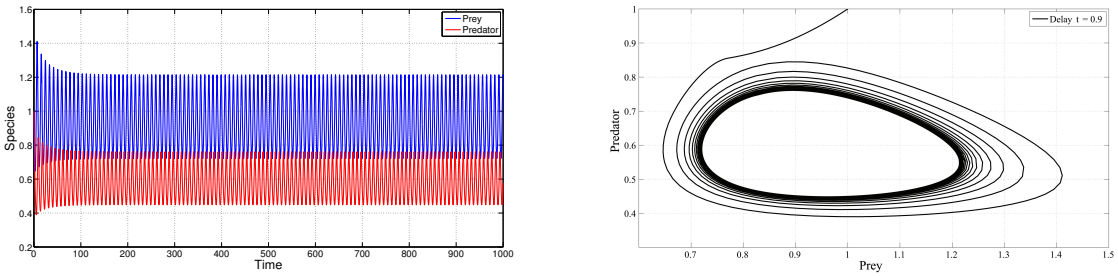

(a) (b)

Figure 8. Taking $\tau = 0.9, \omega = 3.2$ with value of parameters chosen in Q1 with starting point $x(0) = y(0) = 1$, the coexistence equilibrium E_* loses its stability when $m = 0.15 (> 0.07 = m_*)$. Both the Figures (a) and (b) display periodic oscillations and ultimately a stable limit cycle around the E_*.

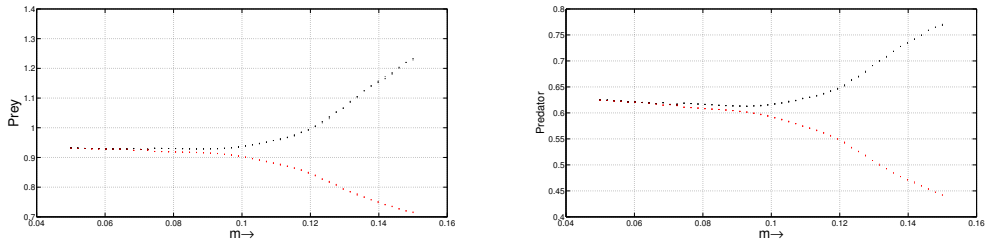

(a) (b)

Figure 9. Diagram illustrating the prey and predator populations' bifurcation in terms of Allee parameter with respect to the bifurcating parameter, m for the parameter set Q1 with starting point $x(0) = y(0) = 1$.

To enhance the applicability of the model in real ecosystems, future work should include parameter estimation based on ecological data and empirical validation to assess the model's predictive accuracy. Further research could also explore evolutionary dynamics explicitly, incorporate additional ecological interactions, and investigate the role of environmental variability and stochastic effects on predator-prey dynamics.

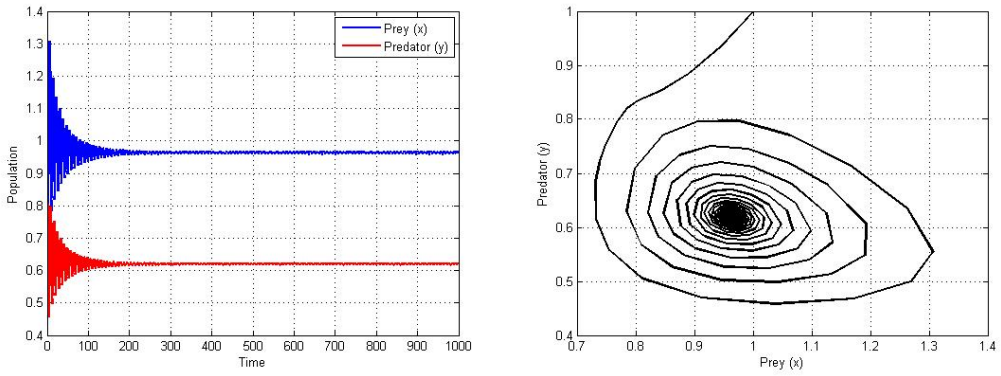

(a) (b)

Figure 10. Taking $\tau = 0.9, \omega = 3.2$ with value of parameters chosen in Q1 with starting point $x(0) = y(0) = 1$, E_* is locally asymptotically stable when harvesting effort $E = 0.4$. (a) The solution graph of x and y of the system (2). (b) The phase space graph of the system (2).

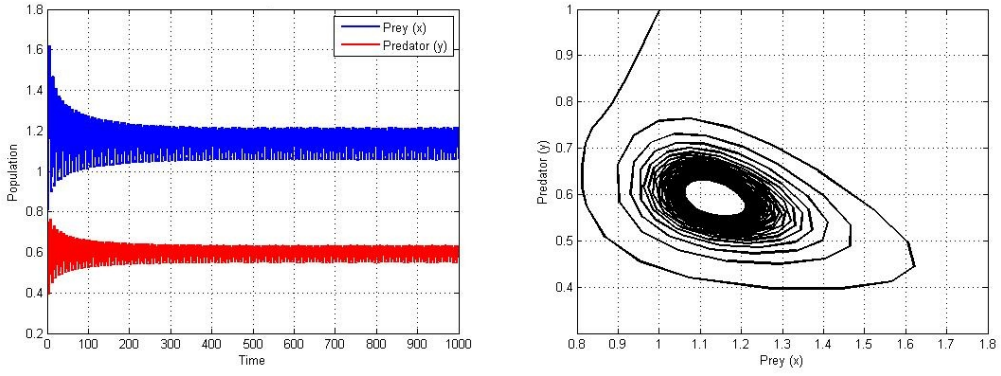

(a) (b)

Figure 11. Taking $\tau = 0.9, \omega = 3.2$ with value of parameters chosen in Q1 with starting point $x(0) = y(0) = 1$, the coexistence equilibrium E_* loses its stability when harvesting effort $E = 0.9$. Both the Figures (a) and (b) display periodic oscillations and ultimately a stable limit cycle around the E_*.

Acknowledgment

The authors would like to express their sincere gratitude to the Faculty of Science and Technology, LPPM Universitas Airlangga, for providing funding support for this research. This work was supported under Research Contract Number: 1777/UN3.LPPM/PT.01.03/2025.

REFERENCES

1. S. Pal, S. Majhi, S. Mandal and N. Pal, Role of Fear in a Predator–Prey Model with Beddington–DeAngelis Functional Response, Zeitschrift für Naturforschung A, 2019, 74(7), 581–595.
2. R. Xue,Y. Shao and M. Cui, Impact of fear and Beddington-DeAngelis functional response in a Predator-Prey Model, International Journal of Mathematics, Statistics and Operations Research, 2023, 3(1), 65-88.

3. P. Majumdar, B. Mondal, S. Debnath, S. Sarkar and U. Ghosh, Effect of fear and delay on a prey-predator model with predator harvesting, Computational and Applied Mathematics, 2022, 41:357.
4. Molla, H., Rahman, Md. S. and Sarwardi, S., 2021, Dynamical study of a prey–predator model incorporating nonlinear prey refuge and additive Allee effect acting on prey species, Modeling Earth Systems and Environment, vol. 7, pp. 749–765.
5. A. L. Firdiansyah, Effect of Fear in Leslie-Gower Predator-Prey Model with Beddington-DeAngelis Functional Response Incorporating Prey Refuge, International Journal of Computing Science and Applied Mathematics, 2021, 7(2), 56-62.
6. A.K. Umrao and P.K. Srivastava, Bifurcation Analysis of a Predator–Prey Model with Allee Effect and Fear Effect in Prey and Hunting Cooperation in Predator, Differential Equations and Dynamical Systems, 2023.
7. B. Xie, Z. Zhang and Na Zhang, Influence of the Fear Effect on a Holling Type II Prey–Predator System with a Michaelis–Menten Type Harvesting, International Journal of Bifurcation and Chaos, 2021, 31(14), 2150216.
8. B. Xie, Impact of the fear and Allee effect on a Holling type II prey–predator model, Advances in Difference Equations, 2021, 464.
9. H. Li and X. Cheng, Dynamics of Stage-Structured Predator–Prey Model with Beddington–DeAngelis Functional Response and Harvesting, Mathematics, 2021, 9(17), 2169.
10. L. Lai, Z. Zhu and F. Chen, Stability and Bifurcation in a Predator–Prey Model with the Additive Allee Effect and the Fear Effect, Mathematics, 2020, 8(8), 1280.
11. S. Vinoth, R. Sivasamy, K. Sathiyanathan, B. Unyong, G. Rajchakit, R. Vadivel and N. Gunasekaran, The dynamics of a Leslie type predator–prey model with fear and Allee effect, Advances in Difference Equations, 2021, 338.
12. S. Pal, P. Panday, N. Pal, A.K. Misraa and J. Chattopadhyay, Dynamical behaviors of a constant prey refuge ratio-dependent prey-predator model with Allee and fear effects, International Journal of Biomathematics, 2024, 17(01), 2350010.
13. K.Q. Al-Jubouri and R.K. Naji, Stability and Hopf Bifurcation of a Delayed Prey-Predator System with Fear, Hunting Cooperative, and Allee Effect, 2024, Iraqi Journal of Science, 65(7), 3901-3921.
14. S. Mondal and G.P. Samanta, Impact of Fear in a Delayed Predator–Prey System with Prey Refuge in Presence of Additional Food, Biophysics, 2021, 66(3), 438–463.
15. Z. Sun and W. Jiang, Bifurcation and Spatial Patterns Driven by Predator-Taxis in a Predator-Prey System with Beddington-DeAngelis Functional Response, Discrete and Continuous Dynamical Systems - Series B, 2024, 29(10), 4043-4070.
16. Vijaya Lakshmi. G.M, Gunasekaran. M, Vijaya. S, Bifurcation Analysis of Prey-Predator Model with Harvested Predator, International Journal of Engineering Research and Development, 2014, 10(6), 42-51.
17. K. Manna and M. Banerjee, Dynamics of a prey–predator model with reproductive Allee effect for prey and generalist predator, Nonlinear Dynamics, 2024, 112, 7727–7748.
18. M. Chen and W. Yand, Effect of Non-Linear Harvesting and Delay on a Predator-Prey Model with Beddington-DeAngelis Functional Response, Commun. Math. Biol. Neurosci, 2024, 2024:26.
19. J.P. Tripathi, S. Abbas and M. Thakur, Dynamical analysis of a prey–predator model with Beddington–DeAngelis type function response incorporating a prey refuge, Nonlinear Dynamics, 2015, 80, 177–196.
20. A. Mapunda and T. Sagamiko, Mathematical Analysis of Harvested Predator-Prey System with Prey Refuge and Intraspecific Competition, 2021, Tanzania Journal of Science, 47(2), 728-737.
21. K. Garain, U. Kumar and P.S. Mandal, Global Dynamics in a Beddington–DeAngelis Prey–Predator Model with Density Dependent Death Rate of Predator, Differential Equations and Dynamical Systems, 2021, 29(1), 265–283.
22. C.A. Ibarra, J.D. Flores and P.V. Heijster, Stability Analysis of a Modified Leslie–Gower Predation Model with Weak Allee Effect in the Prey, Frontiers in Applied Mathematics and Statistics, 2022, 7, Article 731038.
23. P. Kalra, R. Kaur and Aarti, A Prey-Predator Model with Beddington-DeAngelis Holling type IV functional response, Journal of Emerging Technologies and Innovative Research, 2019, 6(1), 452-457.
24. A. Savadogo, B. Sangaré and H. Ouedraogo, A mathematical analysis of Hopf-bifurcation in a prey-predator model with nonlinear functional response, Advances in Difference Equations, 2021, 275.
25. Aldila, D. and Adhyarini, D., A Predator–Prey Model with Fear Factor, Allee Effect and Periodic Harvesting, Proceedings of the 2nd International Conference on Mathematics and Science Education, 2020.
26. Diz-Pita, A. and Otero-Espinar, M., Predator–Prey Models: A Review of Some Recent Advances, Mathematics, 9(15), 1783, 2021.
27. Shao, Y., Yu, H., Jin, C., Fang, Jingzhe and Zhao, Min, Dynamics analysis of a predator-prey model with Allee effect and harvesting effort, Electronic Research Archive 32(10): 5682–5716, 2024.
28. Yang, R. and Jin, D., Dynamics in a predator-prey model with memory effect in predator and fear effect in prey, Electronic Research Archive 30(4): 1322–1339, 2022.
29. Das, S. and Samanta, G.P., Modelling the fear effect in a two-species predator–prey system under the influence of toxic substances, Rendiconti del Circolo Matematico di Palermo, Volume 70, pages 1501–1526, 2021.
30. SHAO, Yuan-fu and ZHAO, Jin-xing, Analysis of Stability and Hopf Bifurcation of a Delayed Predator-prey System with Fear and Additional Food, Acta Mathematicae Applicatae Sinica, English Series, 2025.
31. Lakshmi Narayan Guin, Pallav Jyoti Pal, Jawaher Alzahrani, Nijamuddin Ali, Krishnendu Sarkar, Salih Djilali, Anwar Zeb, Ilyas Khan & Sayed M Eldin, Influence of Allee effect on the spatiotemporal behavior of a diffusive predator–prey model with Crowley–Martin type response function, Nature, 13 (4710), 2023.
32. Guin, L.M., Murmu, R., Baek, H. and Kim, K.H., 2020, Dynamical Analysis of a Beddington–DeAngelis Interacting Species System with Prey Harvesting, Hindawi Mathematical Problems in Engineering, vol. 2020, 22 pages.
33. Hassard BD, Kazarinoff ND, Wan YH. Theory and applications of Hopf bifurcation. Cambridge University Press Cambridge, New York. 1981.
34. Hale JK. and Verduyn Lunel SM. Introduction to Functional Differential Equations. Springer-Verlag, New York. 1993.
35. Song Y. and Wei J. Bifurcation analysis for Chen's system with delayed feedback and its application to control of chaos. Chaos, Solitons and Fractals. 2004.
36. Birkhoff, G.,Rota, G.C. Ordinary Differential Equations. Ginn Boston. 1982.